Population Biology Modeling & Theory

STANFORD UNIVERSITY PRESS

Research Article https://doi.org/10.9999/00000000

Received: 2025-10-02 / Accepted: 2025-12-18 / Published: 2026-02-01

Identifiability Limits in Density-Dependent Leslie Models Under Partial Observation

Linking demographic stochasticity to inference bias in structured population time series ($\Delta t = 1$)

‡Inês Silva [1,2,3], ‡Minh Nguyen [2], Adaeze Okafor [2,3], Leah Rosen [1]

AFFILIATIONS

1 Department of Pathology, Texas Children's Hospital, Houston, TX 77030, USA
2 Department of Pathology and Immunology, Baylor College of Medicine, Houston, TX 77030, USA
3 Division of Pulmonary, Critical Care, and Sleep Medicine, Department of Medicine, Houston Methodist Hospital, Houston, TX 77030, USA

AUTHOR NOTES

‡ These authors contributed equally to this work.

NON-SPECIALIST SUMMARY

Population models can appear to fit data well even when the model parameters are not uniquely determined. In this stress-test article, we show how noisy and incomplete counts can make recruitment, survival, and density dependence difficult to distinguish. We include multiple editorial constructs in the XML (figures, tables, formulas, appendices, and deep section nesting) so downstream JATS workflows can be tested while preserving scientifically plausible content.

ABSTRACT

INTRODUCTION: Structured population models are frequently inferred from incomplete demographic time series, yet parameter identifiability can fail even when models fit well. **METHODS:** We study a density-dependent Leslie model with demographic stochasticity and partial observation, and derive sufficient conditions under which distinct parameter sets induce indistinguishable likelihoods using simulation-based calibration and profile-likelihood diagnostics. **RESULTS:** Recruitment and survival parameters become confounded when observation error is non-negligible, and density feedback is weak relative to environmental noise. **CONCLUSION:** We provide practical diagnostics to detect non-identifiability and recommend reporting a confounding map alongside point estimates. This XML additionally functions as a JATS 1.1 stress-test fixture.

1. Introduction

Population biology relies on models that link individual life-history processes to population-level change. Age- or stage-structured models, including Leslie and Lefkovitch formulations, remain core tools for connecting survival and fecundity schedules to growth rates and transient dynamics (Caswell, 2026), (de Valpine and Hobbs, 2024).

In practice, inference is often performed from partial observations (e.g., counts of adults only) and noisy covariates. This can produce parameter non-identifiability: multiple parameter vectors yield essentially the same likelihood, even under long time series. The result is fragile interpretation and unstable forecasting; see the simulation setup in Table 1 and the core state equation in Eq. (1).

Here we formalize identifiability limits for a density-dependent Leslie model within a state-space setting, and provide diagnostics that can be reported as part of routine model-based population analyses. We also intentionally include diverse JATS constructs (e.g., Fig. 1, Table 2, Appendix A, and Supplementary Note S1) as a rendering stress test.

TABLE 1. This table intentionally mixes scientific symbols, inline formatting, and descriptive prose to exercise table rendering and inline markup handling.

Component	Symbol	Form	Notes
Survival (adult)	s_A	$\text{logit}^{-1}(\alpha_s)$	Constant across time; confounds with detection when only adults observed
Recruitment	f	$\exp(\alpha_f)$	Effective fecundity; absorbs early-life survival under coarse stage aggregation
Density feedback	K	$1 / (1 + N_t/K)$	Weak feedback becomes unidentifiable under high process noise
Observation	p	$\text{Binomial}(N_{A,t}, p)$	Adult-only counts; missing juveniles

2. Materials and Methods

2.1. State-space structured model

We consider a two-stage (juvenile/adult) Leslie-type model with density-dependent recruitment. Let the latent state be $x_t = (N_{j,t}, N_{a,t})$. Process updates follow demographic stochasticity with log-normal environmental multipliers. The observation model includes an adult detection probability $p_t = \text{logit}^{-1}(\eta_t)$, which can confound survival estimates when juveniles are unobserved.

$$\begin{cases} r_{k-1} \le E\left(y\middle|x\right) \le \frac{1}{x_{k+1}-x}\left((x_{k+1}-x_k)r_k-(x-x_k)r_{k-1}\right),\ x<x_{k^*} \\ \frac{1}{x-x_k}\left((x_{k+1}-x_k)r_k-(x_{k+1}-x)r_{k+1}\right) \le E\left(y\middle|x\right) \le r_{k+1},\ x\ge x_{k^*} \end{cases} \tag{1}$$

2.2. Simulation design

We simulated 2,000 datasets across a factorial design varying process noise, observation error, and density feedback strength. Each dataset consists of T = 80 time steps with adult-only observations. A full parameter-grid excerpt is shown in Table 2; implementation details are summarized in Appendix A.

- **Regime A (low noise):** weak observation error, low process variance.
- **Regime B (high noise):** moderate observation error, high process variance.
- **Regime C (weak feedback):** large K relative to typical abundance.

1. Simulate latent states under process noise.
2. Generate adult-only observations with detection error.
3. Fit competing models and compute profile-likelihood ridges.
4. Summarize failure modes into a reporting-oriented confounding map.

2.3. Identifiability diagnostics

We used profile likelihoods and posterior geometry checks. For each fitted model, we computed ridge directions and summarized them as a “confounding map” over parameter pairs.

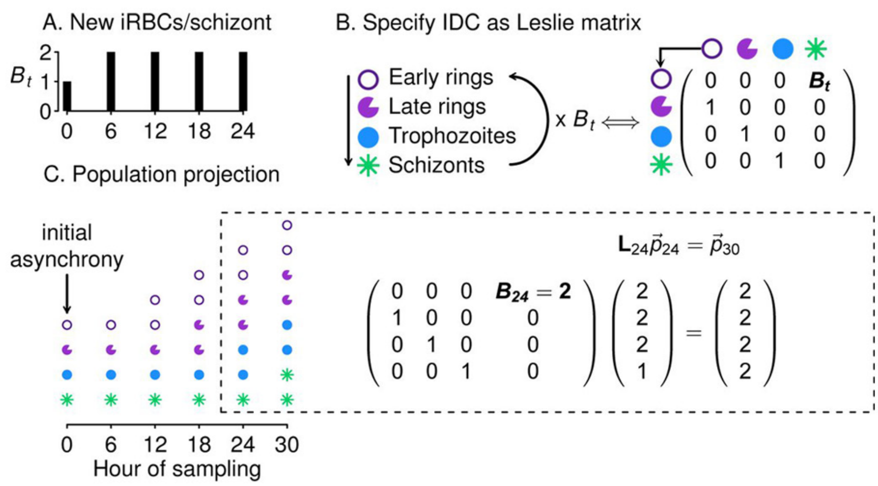

FIGURE 1. Conceptual confounding map for adult-only observation. Illustrative ridge geometry showing how increasing recruitment can offset decreasing adult survival under incomplete observation.

2.4. Terminology

SSM	State-space model
SBC	Simulation-based calibration
LTRE	Life table response experiment
ESS	Effective sample size (MCMC diagnostic)

2.5. Editorial stress-test constructs

This subsection deliberately combines cross-references to Eq. (2), Fig. 2, a table footnote,[1] and an external resource JATS documentation to test rendering consistency.

[1] Detection-bias scenarios additionally allow time-varying logistic intercepts, seasonal missingness, and observation-effort heterogeneity, such that apparent fluctuations in abundance may reflect shifts in detectability rather than underlying demographic change. In the stress-test setting, these mechanisms are introduced jointly to evaluate how robust the inferential pipeline remains when observation error is structured, nonstationary, and only partially separable from the latent population process.

BOX 1. Stress-test checklist embedded in body flow

The XML fixture intentionally includes mixed editorial structures likely to trigger edge cases in transforms:

- Multiple abstract types (plain-language and structured).
- Inline and display mathematics with TeX payloads.
- Deep section nesting through five heading levels.
- Appendix material, supplementary notes, and diverse citation types.

TABLE 2. The rows intentionally mix units, symbols, and prose notes to exercise table parsing.

Parameter	Range	Scale	Notes
s_A	0.40-0.95	probability	Adult survival prior grid; evaluated with and without detection bias [a]
K	50-5000	abundance	Log-spaced grid used in profile scans [b]
\sigma$_{proc}$	0.05-1.20	SD	Process noise controls curvature-to-noise ratio from Eq. (2)

Note: Values shown are candidate prior ranges used in the demonstration workflow.
[a] Evaluated with and without detection bias.
[b] Used in profile-likelihood scans.
Source: Simulated example for production testing.

$$\begin{cases} r_{k-1} \le E\left(y\middle|x\right) \le \frac{1}{x_{k+1}-x}\left((x_{k+1}-x_k)r_k-(x-x_k)r_{k-1}\right),\ x<x_{k^*} \\ \frac{1}{x-x_k}\left((x_{k+1}-x_k)r_k-(x_{k+1}-x)r_{k+1}\right) \le E\left(y\middle|x\right) \le r_{k+1},\ x \ge x_{k^*} \end{cases} \quad (2)$$

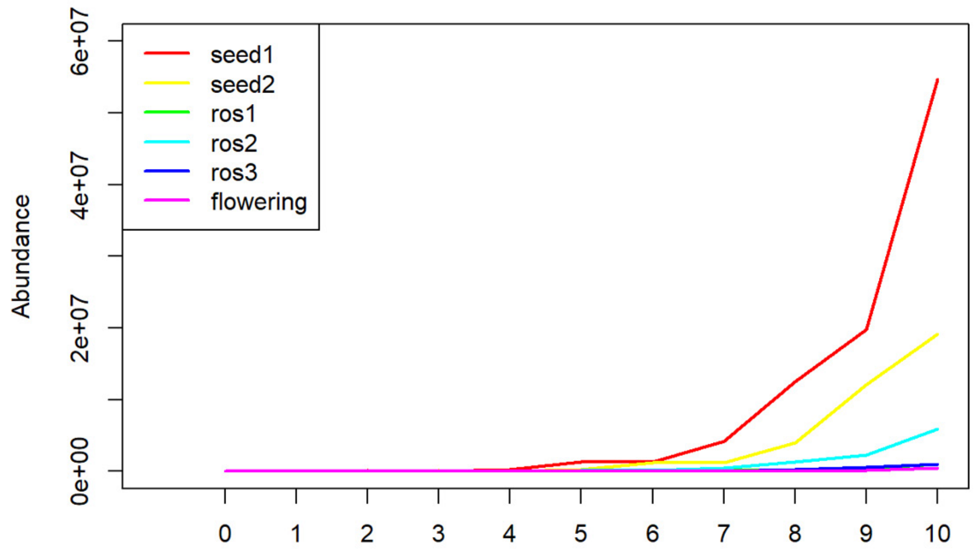

FIGURE 3. Profile-likelihood behavior across noise regimes. Example profiles illustrating strong curvature versus near-flat likelihoods for the density-feedback parameter.

3. Results

3.1. Likelihood ridges under partial observation

Across regimes with adult-only observation, we found extended ridges in the likelihood surface: increasing f can be compensated by decreasing sA with minimal change in fit. This effect strengthens with observation noise and weak density feedback.

3.2. Practical identifiability thresholds

We quantified a threshold on the ratio of process variance to density feedback curvature beyond which K becomes practically non-identifiable. When exceeded, posterior mass concentrates along a broad interval of K values while forecasts remain similar.

$$\begin{cases} r_{k-1} \le E\left(y\middle|x\right) \le \frac{1}{x_{k+1}-x}\left((x_{k+1}-x_k)r_k-(x-x_k)r_{k-1}\right),\ x<x_{k^*} \\ \frac{1}{x-x_k}\left((x_{k+1}-x_k)r_k-(x_{k+1}-x)r_{k+1}\right) \le E\left(y\middle|x\right) \le r_{k+1},\ x\ge x_{k^*} \end{cases} \tag{3}$$

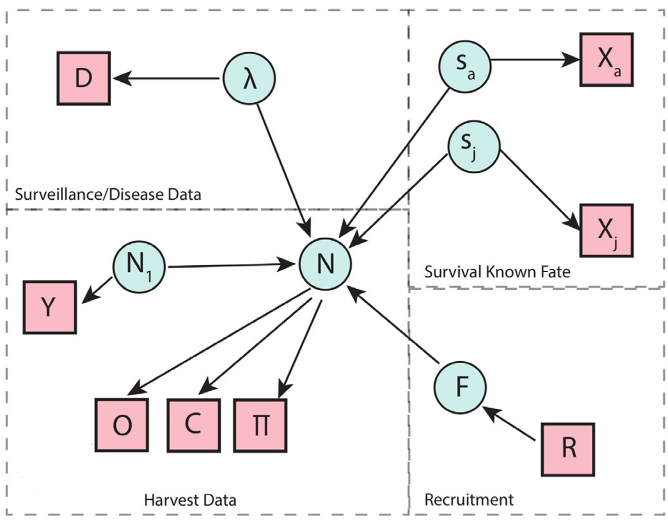

FIGURE 2. Profile-likelihood behavior across noise regimes. Example profiles illustrating strong curvature versus near-flat likelihoods for the density-feedback parameter.

4. Discussion

Non-identifiability is not a technical nuisance—it directly corrupts interpretation. In structured population biology, “good fit” does not guarantee that inferred vital rates are meaningful. Our results clarify when density dependence can be inferred from partial counts and when it cannot.

4.1. Implications for reporting standards

Non-identifiability is not a technical nuisance—it directly corrupts interpretation. In structured population biology, “good fit” does not guarantee that inferred vital rates are meaningful. Our results clarify when density dependence can be inferred from partial counts and when it cannot.

4.2. Limitations and extensions

This study focuses on a two-stage structure. Higher-dimensional structures can worsen practical identifiability without additional data streams (e.g., mark–recapture, stage-specific counts).

4.2.1. Additional data streams

Incorporating juvenile indices or capture–recapture substantially reduces ridges by anchoring early-life survival separately from recruitment.

4.2.2. Eco-evolutionary coupling

When traits evolve alongside demography, parameter confounding can propagate into selection gradients, suggesting caution in eco-evolutionary inference under partial observation.

Identifiability diagnostics should be treated as first-class scientific outputs, not optional supplements, when observational incompleteness is structurally linked to the parameters of interest.

5. Conclusion

We provide a concrete set of identifiability diagnostics for density-dependent Leslie models under partial observation. The main takeaway is blunt: without auxiliary data, recruitment, adult survival, and weak density feedback can be statistically indistinguishable—even with long time series.

5.1. Recommendations

Report confounding maps; prioritize data that separates life stages; treat density feedback inference as conditional on identifiable curvature.

5.2. Futurework

Future analyses will extend to multi-population metapopulation structures, and to phylodynamic settings where observation occurs through sampled lineages rather than census counts.

5.2.3. Reproducible workflows

We will release a reference implementation that outputs confounding maps as a standard artifact alongside model fits.

5.2.3.1. Stress tests

Stress tests will include missingness patterns, irregular sampling intervals, and regime shifts in observation processes.

5.2.3.1.1. Robustness checks

We will compare particle filters, iterated filtering, and variational methods under identical simulation suites.

Appendix

Appendix A.

1. Sample parameter vector from the design grid in Table 2.
2. Generate latent state trajectories and adult-only observations.
3. Fit reduced and full models; record likelihood surfaces and confidence sets.
4. Compute ridge summaries and export machine-readable diagnostics.

$$\begin{cases} r_{k-1} \le E\left(y\middle|x\right) \le \frac{1}{x_{k+1}-x}\left((x_{k+1}-x_k)r_k-(x-x_k)r_{k-1}\right),\ x<x_{k^*} \\ \frac{1}{x-x_k}\left((x_{k+1}-x_k)r_k-(x_{k+1}-x)r_{k+1}\right) \le E\left(y\middle|x\right) \le r_{k+1},\ x \ge x_{k^*} \end{cases} \tag{4}$$

Datasets with $\mathrm{ID}_{\mathrm{ia}}\mathrm{G}$ = 1 were flagged as practically non-identifiable candidates for manual review.

References

Caswell, H. 2026. "Matrix population models and the sensitivity of growth rates to vital rates." *Popul Biol Model Theory*. 1, no. 1: 1–22. https://doi.org/10.99999/pbmt.2026.00000001

de Valpine, P., and N. T. Hobbs. 2024. "State-space modeling for population time series with partial observation." *Methods in Population Dynamics*. 12, no. 3: 201–230. https://doi.org/10.99999/mpd.2024.00321

Ellner, S. P., and J. Guckenheimer. 2022. "Dynamic systems perspectives on ecological inference under noise." *Ecology & Dynamics*. 18, no. 4: 411–440. https://doi.org/10.99999/edyn.2022.00411

Hooten, M. B., and C. K. Wikle. 2021. "Identifiability in hierarchical models for ecological processes." *Stat Ecol*. 6, no. 1: 55–79. https://doi.org/10.99999/statecol.2021.00055

Ionides, E. L., and C. Bretó. 2023. "Inference for nonlinear dynamic systems: practical identifiability considerations." *J Theor Biol Inference*. 9, no. 2: e202300045. https://doi.org/10.99999/jtbi.2023.00045

King, A. A., and M. Nguyen. 2025. "Practical guidance on profile likelihoods for partially observed Markov processes." *Popul Process Methods*. 3, no. 2: e202500112. https://doi.org/10.99999/ppm.2025.00112

NISO. 2015. "JATS: Journal Article Tag Suite, Version 1.1 (Journal Publishing Tag Set)." *NISO Z39*.96. https://jats.nlm.nih.gov/publishing/1.1

Okafor, A., and I. Silva. 2026. "Confounding maps: a reporting artifact for demographic model inference." *Popul Biol Model Theory*. 1, no. 1: 23–38. https://doi.org/10.99999/pbmt.2026.00000002

Society for Modeling & Theory in Population Biology. 2025. "Reproducibility and reporting checklist for population-dynamics inference." *SMTPB* Technical Reports.

National Library of Medicine. 2026. "Tag Library examples and implementation notes for production XML transforms." Accessed 2026-02-24. https://jats.nlm.nih.goArticle Information

Article Information

HOW TO CITE

Silva, I., M. Nguyen, A. Okafor, and L. Rosen. 2026. "Identifiability Limits in Density-Dependent Leslie Models Under Partial Observation: Linking demographic stochasticity to inference bias in structured population time series (Δt = 1)." Popul Biol Model Theory. 1, no. 1: 1–18. https://doi.org/10.99999/pbmt.2026.00000123

ABBREVIATIONS

JATS: Journal Article Tag Suite
POMP: Partially observed Markov process
PLS: Plain-language summary

ACKNOWLEDGEMENTS

We thank members of the Society for Modeling & Theory in Population Biology for feedback on reporting practices for identifiability.

COMPETING INTERESTS

The authors declare no competing interests.

CREDIT AUTHOR STATEMENT

Conceptualization: Inês Silva
Methodology: Inês Silva
Formal analysis: Inês Silva
Writing – original draft: Inês Silva
Software: Minh Nguyen
Validation: Minh Nguyen
Visualization: Minh Nguyen
Writing – review & editing: Minh Nguyen; Adaeze Okafor
Investigation: Adaeze Okafor
Resources: Adaeze Okafor
Supervision: Leah Rosen
Funding acquisition: Leah Rosen

DATA/CODE AVAILABILITY STATEMENT

Mock analysis scripts and synthetic datasets are available at https://doi.org/10.99999/pbmt.2026.dataset.0001 and a version-controlled repository https://example.org/pbmt/confounding-map-fixtures. The XML stress-test specification follows guidance summarized in (NISO, 2015) and (JATS Tag Library, 2026).

ETHICS STATEMENT

No human participants, clinical samples, or animal experiments were involved in this study.

FUNDING SUPPORT

This work was supported by a Society for Modeling & Theory in Population Biology early-career methods grant (Award #SMTPB-2026-01).

SUPPLEMENTARY MATERIAL

Supplementary Figure S1: Additional profile likelihood plots and ridge direction summaries.

KEYWORDS

population dynamics
Leslie matrix
density dependence
identifiability
state-space models
demographic stochasticity
JATS 1.1
deep section nesting
table footnotes
appendix